

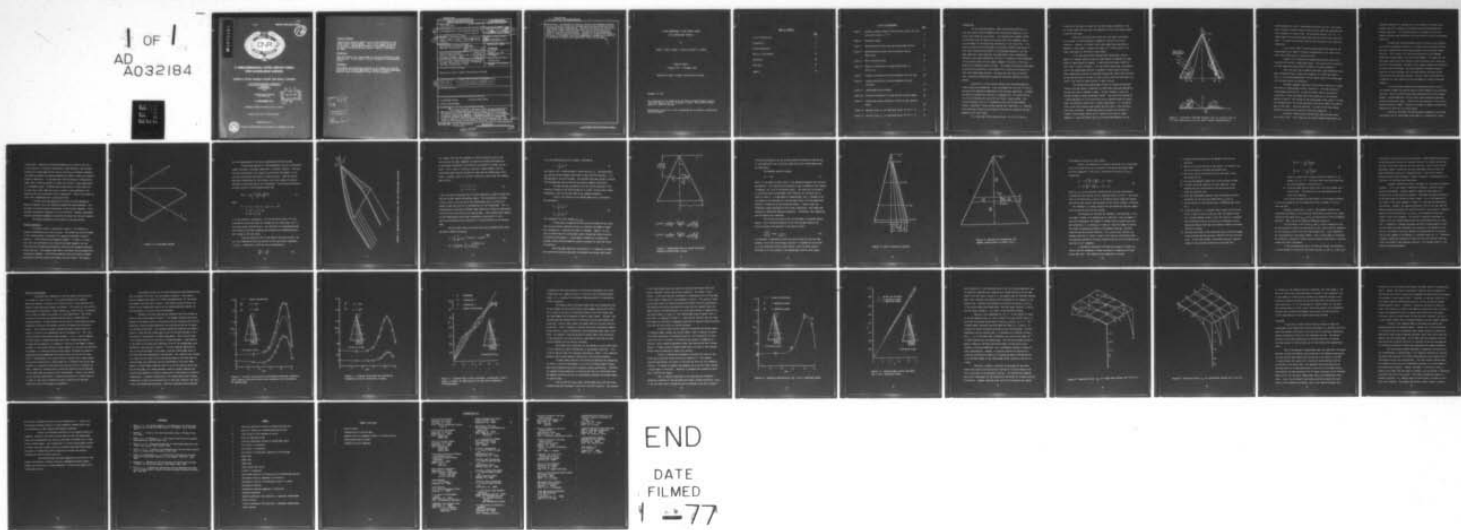
AD-A032 184 MASSACHUSETTS INST OF TECH CAMBRIDGE FLUID DYNAMICS --ETC F/G 20/4
A THREE-DIMENSIONAL LIFTING SURFACE THEORY WITH LEADING-EDGE VO--ETC(U)
DEC 75 T K MATOI, E E COVERT, S E WIDNALL N00014-75-C-0257

UNCLASSIFIED

ONR-CR215-230-2

NL

1 OF 1
AD A032184



END

DATE
FILMED

1 -77

AD A032184

REPORT ONR-CR215-230-2

FG.
12



A THREE-DIMENSIONAL LIFTING SURFACE THEORY WITH LEADING-EDGE VORTICES

THOMAS K. MATOI, EUGENE E. COVERT AND SHEILA E. WIDNALL

FLUID DYNAMICS RESEARCH LABORATORY ✓
MASSACHUSETTS INSTITUTE OF TECHNOLOGY
CAMBRIDGE
MASSACHUSETTS
02139

CONTRACT N00014-75-C-0257
ONR TASK 215-230

31 DECEMBER 1975

D D C
RECORDED
NOV 17 1976
REF ID: A64120
B

TECHNICAL REPORT FOR PERIOD 1 JAN 75 - 31 DEC 75

Prepared for public release; distribution unlimited.

PREPARED FOR THE



OFFICE OF NAVAL RESEARCH • 800 N. QUINCY ST. • ARLINGTON • VA • 22217

Change of Address

Organizations receiving reports on the initial distribution list should confirm correct address. This list is located at the end of the report. Any change of address or distribution should be conveyed to the Office of Naval Research, Code 211, Washington, DC 22217.

Disposition

When this report is no longer needed, it may be transmitted to other organizations. Do not return it to the originator or the monitoring office.

Disclaimer

The findings and conclusions contained in this report are not to be construed as an official Department of Defense or Military Department position unless so designated by other official documents.

ACCESSION NO.	
NTIS	White Section <input checked="" type="checkbox"/>
DEC	Buff Section <input type="checkbox"/>
UNARMED	
JUSTIFICATION	
BY	
DISTRIBUTION/AVAILABILITY CODES	
Dist.	AVAIL. REG OR SPECIAL
A	

~~UNCLASSIFIED~~

~~SECURITY CLASSIFICATION OF THIS PAGE (When Data Entered)~~

DD FORM 1 JAN 73 1473 EDITION OF 1 NOV 68 IS OBSOLETE
S/N 0102-014-6601

Unclassified

in which

SECURITY CLASSIFICATION OF THIS PAGE (When Data Entered)

140250

Unclassified

SECURITY CLASSIFICATION OF THIS PAGE(When Data Entered)

coefficients. The unknowns are found by satisfying the downwash condition, the Kutta condition at the trailing edge and the no-force condition on the leading-edge vortex representation. The Kutta condition is now nonlinear in terms of the unknown vorticity coefficients and is satisfied by direct iteration in a quasi-linearized form. The position of the leading-edge vortex is found by applying a Newton's procedure to eliminate the forces on the vortex. Preliminary results and suggestions to enhance the versatility of the method by reducing the computational effort are presented.

SECURITY CLASSIFICATION OF THIS PAGE(When Data Entered)

A THREE-DIMENSIONAL LIFTING SURFACE THEORY
WITH LEADING-EDGE VORTICES

by

Thomas K. Matoi, Eugene E. Covert and Sheila E. Widnall

Technical Report

1 January 1975 - 31 December 1975

Approved for public release; distribution unlimited.

December 31, 1975

This investigation was supported by the Office of Naval Research, Vehicle Technology Program, Code 211, Arlington, Virginia 22217, under Contract N00014-75-C-0257 (NR 215-230).

Reproduction in whole or in part is permitted for any purpose of the United States Government.

TABLE OF CONTENTS

	<u>Page</u>
List of Illustrations	2
Introduction	3
Problem Formulation	8
Results of the Program	22
Conclusion	34
References	37
Symbols	38

LIST OF ILLUSTRATIONS

	<u>Page</u>
Figure 1. Schematic sketches showing flow on suction side of 70° flat plate delta wing at $\alpha \approx 15^\circ$	5
Figure 2. Coordinate system.	9
Figure 3. Representation of wing, wake and leading-edge vortices	11
Figure 4. Representation of bound vorticity feeding leading-edge vortex	14
Figure 5. Wing collocation points	16
Figure 6. Regions of integration for upwash coefficients at point (x,y)	17
Figure 7. Loading calculated by satisfying downwash condition only	24
Figure 8. Loading calculated by satisfying downwash and Kutta conditions	25
Figure 9. Leading-edge vortex strength	26
Figure 10. Pressure distribution for three and four spanwise modes.	29
Figure 11. Leading-edge vortex strength for three and four spanwise modes	30
Figure 12. Spanwise force, F_y , on right-hand vortex for $\Gamma(1) = .31$	32
Figure 13. Vertical force, F_z , on right-hand vortex for $\Gamma(1) = .31$	33

Introduction

The low speed performance, safety and handling qualities of a high span loading aircraft depend on the structure and stability of the vortex flow created by the aircraft. In a previous work by Matoi (1975)¹, a preliminary study was made of the various flow field components and of existing models of the wing-vortex interactions in the entire flow. This study has shown that existing models are severely limited to the extent to which they incorporate the effects of leading-edge separation, trailing-edge separation, vortex bursting, and complicated flight configurations. Therefore, the present program was initiated to formulate a three-dimensional lifting surface theory for the steady, symmetric flow about a flat plate delta wing at moderate angles of attack. This simple problem was investigated to ensure the tractability of the problem while retaining the features of flows with leading-edge vortices. The study was restricted to the near field vortex-wing interactions although the techniques employed are quite general.

Historically, lifting surface theories have been developed with several underlying assumptions. First one assumes that the flow is inviscid outside of the immediate neighborhood of the wing-body combination. Secondly, one generally assumes that the flow is incompressible. The second restriction can be eliminated by scaling for the linear, steady problem. This solution procedure can also be extended to solve the unsteady problem. Finally, traditional lifting surface theories are linearized, i.e., perturbation velocities created by the presence of the wing are assumed to be small compared to the free stream.

In a linearized lifting surface theory, the lift is linear as

a function of the angle of attack for the small angles considered. Also, the linear formulation precludes the formation of free vortex sheets except at the trailing edge.

These are reasonable restrictions for high aspect ratio wings at low angles of attack employed on commercial aircraft and military transports. However, for fighters with highly swept wings operating at moderate to high angles of attack, this model of a lifting surface is no longer applicable for the entire flight regime.

It has been historically observed that leading-edge vortices appear at a moderate angle of attack of approximately 10 degrees for sweep angles of approximately 60 degrees. A description by Örnberg (1954)² of such a flow is given in Figure 1. For less highly swept wings, the formulation of the leading-edge vortices is delayed to higher angles of attack. These leading-edge vortices are important because they induce high velocities on the wing and control surfaces in their vicinity, and they also affect the overall flow field for other aircraft in their vicinity.

The problem with leading-edge vortices has aroused considerable interest with the advent of supersonic aircraft where sweep was employed to decrease the drag at supersonic speeds. An early attempt to study this problem was made by Brown and Michael (1955)³. They solved the problem for a simplified model of a flat plate delta wing at moderate angles of attack under the additional restriction of slender body theory, i.e., the derivatives in the flow direction were ignored and only those in the transverse plane were considered. Slender-body theory precludes the inclusion of subsonic trailing-edge effects and is limited to the study of simple geometries. Brown and Michael used the following approximation for the

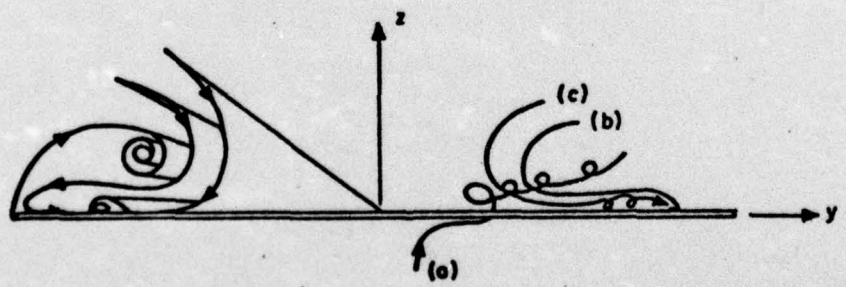
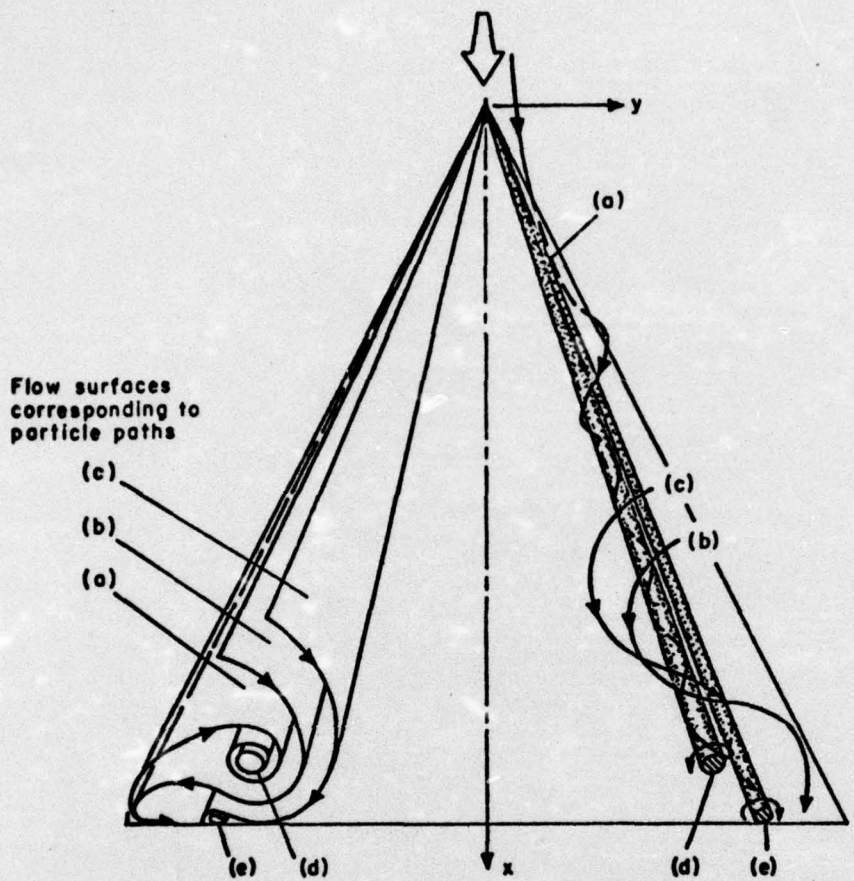


Figure 1. Schematic sketches showing flow on suction side of 70° flat plate delta wing at $\alpha=15^\circ$ [after Örnberg (1954)].

leading-edge vortex sheet. They modeled the vortex core by a line vortex whose strength increased linearly along its axis, which was consistent with their assumption of conical flow. The vortex was fed by a cut, i.e., a feeding sheet from the leading edge which was restricted to the cross-flow plane. This model of the vortex sheet will be referred to as a vortex-cut combination.

Later, Smith (1966)⁴ refined the Brown and Michael model of the leading-edge vortex sheet to include a representation of an actual force-free vortex sheet as well as the vortex core.

However, all of these early presentations had the restrictive assumptions of conical, slender body theory. The restriction of conicality has been removed by Smith (1957)⁵ and others for several geometries.

Thus, the final step in modeling the fully three-dimensional wing-body configuration was to remove the assumption of slender body theory. That is, a fully three-dimensional lifting surface theory with leading-edge vortices would have to be formulated.

To extend standard linearized lifting surface theories to include the effects of leading-edge vortices, one must 1) allow the presence of leading-edge vortices and 2) include non-linear terms in the pressure calculations. These two changes add to the complexity of the original problem in that 1) the location of the leading-edge vortex sheets is originally unknown and 2) for a given location of the vortex sheets, the requirement of zero load -- the Kutta condition -- at the trailing edge becomes nonlinear in terms of the velocity or vorticity components.

Linearized lifting surface theories have been developed along two distinct lines. First, there are the finite element methods where the

wing-body combination is replaced by a finite number of discrete vortex elements and their strengths are determined by satisfying appropriate boundary conditions. The alternate method is to employ a finite set of loading functions whose coefficients are then chosen to satisfy the boundary conditions.

Although the linearized method based on discrete vortex elements has received considerable attention, it contains several inherent disadvantages when compared with the alternate approach using continuous loading functions. First, there is an infinite discontinuity in the downwash between the discrete panels or at the vortex element. This makes the solution highly sensitive to the location of the collocation points where the velocity is being matched. Secondly, finite element methods have traditionally had stability problems. Artifices have been introduced to ensure stability in given instances, but such modifications introduce further arbitrariness into the final solution. Finally, there is the difficulty in modeling the local behavior at the wing edges by a choice of discrete elements.

For the nonlinear problem with leading-edge vortices, one can also attempt to model the wing and wake by finite elements or by continuous functions. Due to the difficulties often encountered with finite element methods, a three-dimensional lifting surface theory employing continuous loading functions was sought. Previous work has been done in this area by Nangia and Hancock (1968).⁶ Therefore, the model of Nangia and Hancock was employed as a basis for this investigation.

Basically, the Nangia and Hancock model attempted to add a Brown and Michael type of leading-edge vortex model to a conventional lifting

surface model. Whereas the linearized problem can be solved in one step as the solution of a system of simultaneous linear equations, the nonlinear problem with leading-edge vortices must be solved by an iterative procedure. The method that Nangia and Hancock employed was simple in theory but required extensive computation. It was hoped that with the advance of computational speed, that it would be possible to reduce the original lengthy computations to a reasonable length. Although several deficiencies of their model will be noted later, their model was used as a basis to take advantage of the expertise that they had gained in their computations. Some of the efforts to refine their computations will be discussed later.

The basic governing equations are similar to those employed by Nangia and Hancock, but a new iterative procedure has been developed. This was done to alleviate several shortcomings in the original procedure. First, the Nangia and Hancock procedure is not self-starting. Secondly, the method requires considerable judgment in selecting the values for the next iteration.

The present formulation will be given in the next section.

Problem Formulation

The choice of axes is presented in Figure 2. The planform is presently considered to be in the x-y plane. The problem can also be treated if the lifting surface is non-planar if a spanwise coordinate is used to replace y. The planform can be completely general. If there is no side-slip, the clean configuration can often be considered symmetric and the flow field can be completely described by satisfying the boundary conditions on one side only. The boundary conditions on the other side are automatically satisfied by symmetry. To facilitate comparison with the results of Nangia and Hancock, the delta wing of unit aspect ratio was chosen. See Figure 3

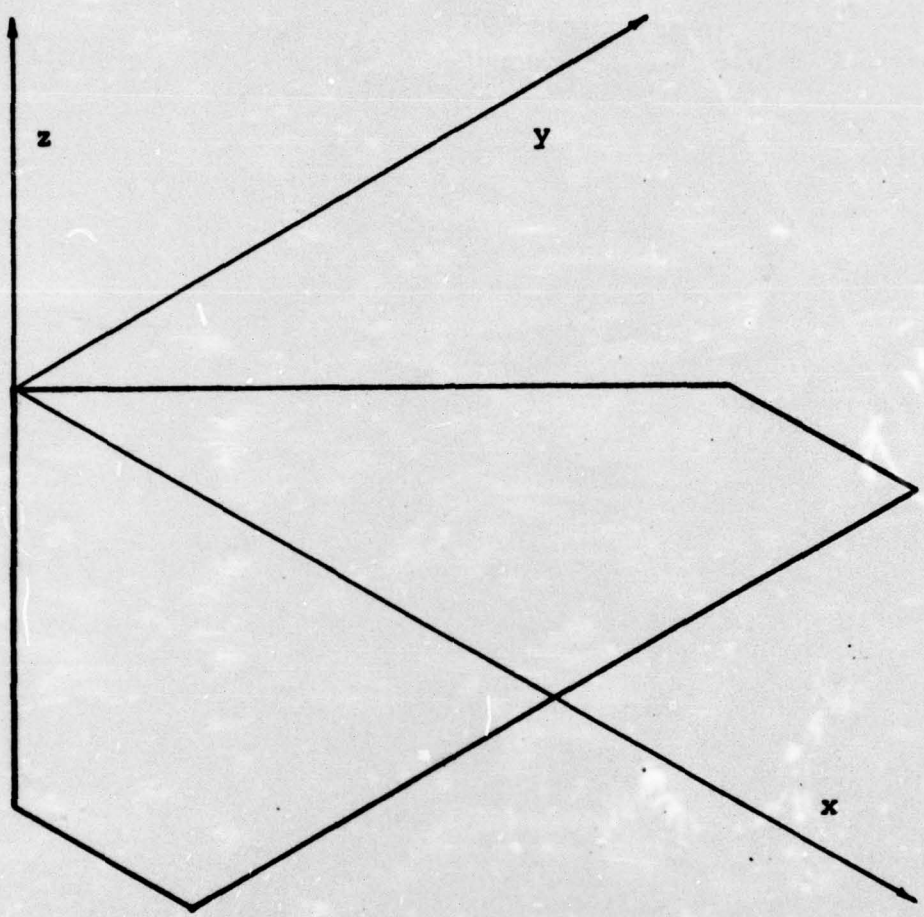


Figure 2. Coordinate system.

for the representation of the wing, leading-edge vortices and wake.

The governing equation in three-dimensional inviscid, irrotational, steady flow about a wing-body combination is Laplace's equation. The solution can be formulated as an integral equation over the boundary of the aircraft configuration and regions of shed vorticity. There are several equivalent formulations for the solution, but vortex sheets are used to represent the wing and wake in this formulation. The velocity distribution can then be given in the following vector form

$$\vec{v}(\vec{r}) = -\frac{1}{4\pi} \int_{S'} \frac{\vec{\gamma} \times (\vec{r}' - \vec{r}) dS'}{|\vec{r}' - \vec{r}|^3} \quad (1)$$

where

$$\begin{aligned}\vec{r}' - \vec{r} &= (x' - x)\hat{i} + (y' - y)\hat{j} + (z' - z)\hat{k} \\ \vec{\gamma} &= \gamma_x \hat{i} + \gamma_y \hat{j} + \gamma_z \hat{k} \\ \vec{v} &= u\hat{i} + v\hat{j} + w\hat{k}\end{aligned}$$

S' is the surface of integration, $\vec{\gamma}$ is the vorticity vector, \vec{v} is the perturbation vector which does not include the unit free stream, and \vec{r} is the radius vector from the origin. The velocities are nondimensionalized with respect to the free stream and the distances are nondimensionalized with respect to the root chord.

Since the vorticity lies in the plane of the wing and wake, the vorticity representing the wing consists of only two nonzero components, γ_x and γ_y . Continuity of vorticity can be represented by

$$\frac{\partial \gamma_y}{\partial y} = -\frac{\partial \gamma_x}{\partial x} \quad (2)$$

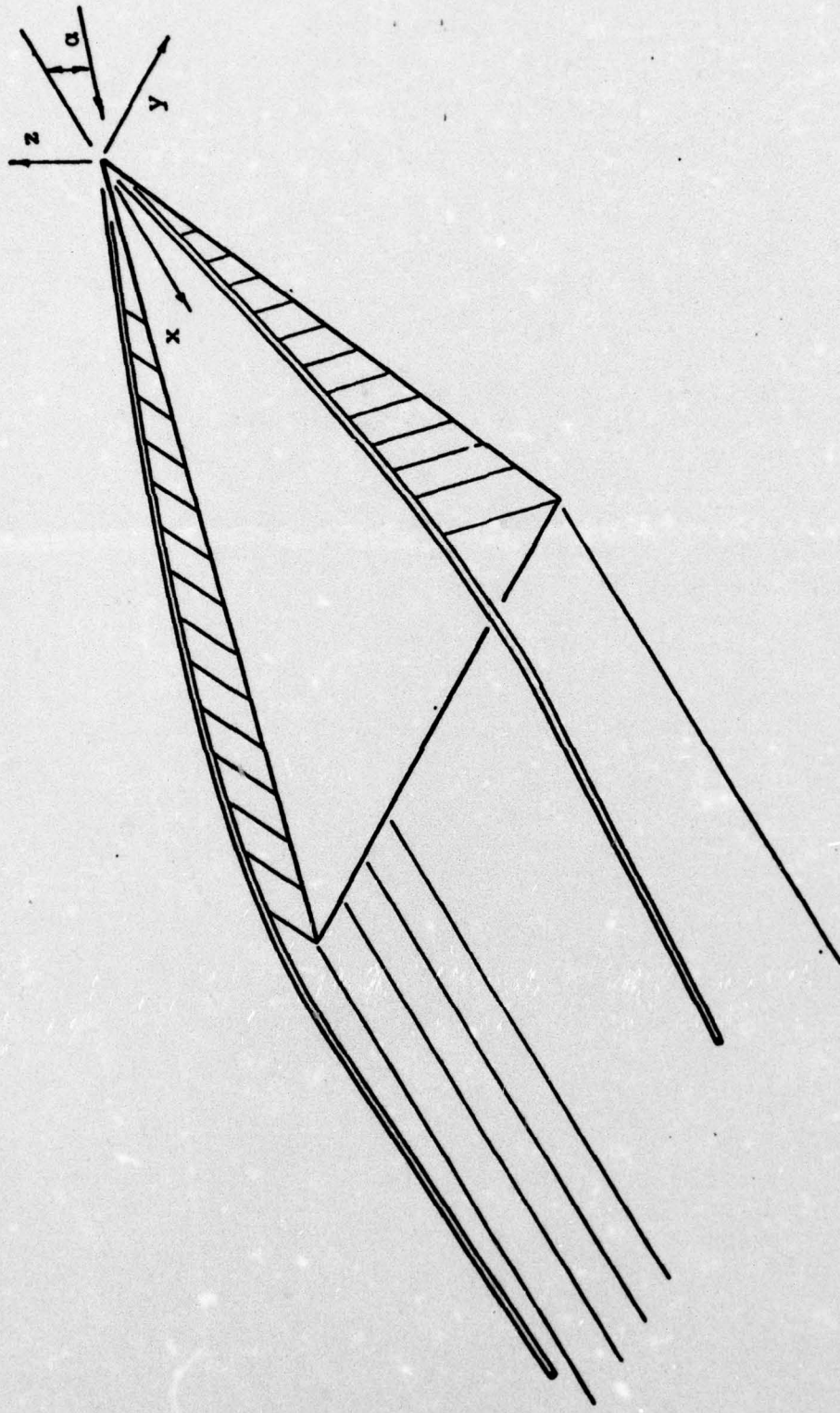


Figure 3. Representation of wing, wake and leading-edge vortices.

This implies that only one component of vorticity need be given on the wing and that the other component can then be calculated from Equation 2. In the present formulation, the vorticity on the wing is divided into two parts. First, there is a portion--subscript 1--which behaves like the traditional bound vortices and does not feed into the leading-edge vortex sheets. Secondly, there is a portion--subscript 2--which feeds the leading-edge vortices.

$$\begin{aligned}\gamma_y &\equiv \gamma = \gamma_1 + \gamma_2 \\ \gamma_x &\equiv \delta = \delta_1 + \delta_2\end{aligned}\quad (3)$$

γ and δ are used to represent the vorticity components to simplify comparison with the original Nangia and Hancock report. The contributions are chosen so that γ_1 and δ_1 fall to zero at the leading edge, while γ_2 and δ_2 are chosen so that the vorticity is perpendicular to the leading edge. This is necessitated by the Brown and Michael model employing a vortex-cut combination to ensure finite velocities at the leading edge. A more general model employing the leading-edge vortex sheet formulated by Smith would utilize a vorticity distribution which resulted in a no-load condition at the leading edge.

The functional forms of the wing vorticity are modeled after those employed by Nangia and Hancock.

$$\begin{aligned}\delta_1 &= \sum_{p=0}^n \sum_{q=0}^m a_{p,q} x^q (y/kx) (1 - (y/kx)^2)^{\frac{2p+1}{2}} \\ \delta_2 &= \frac{x}{(x^2+y^2)^{1/2}} \sum_{q=1}^l g_q q \left[\frac{x^2+y^2}{1+k^2} \right]^{(q-1)/2}\end{aligned}\quad (4)$$

while the leading-edge vortex strength is defined by

$$\Gamma = \sum_{q=1}^k g_q x^q \quad (5)$$

See Figure 4 for a representation of bound vorticity δ_2 . The coefficients $a_{p,q}$ and g_q are the unknown coefficients of the vorticity functions. k is the semispan at the trailing edge. The functions have been chosen to satisfy the aforementioned restrictions and the obvious symmetry constraints.

The wake has been considered to be flat and an extension of the vorticity strength at the trailing edge as in linear lifting surface theory. Consequently, the trailing wake adds no new unknown parameters.

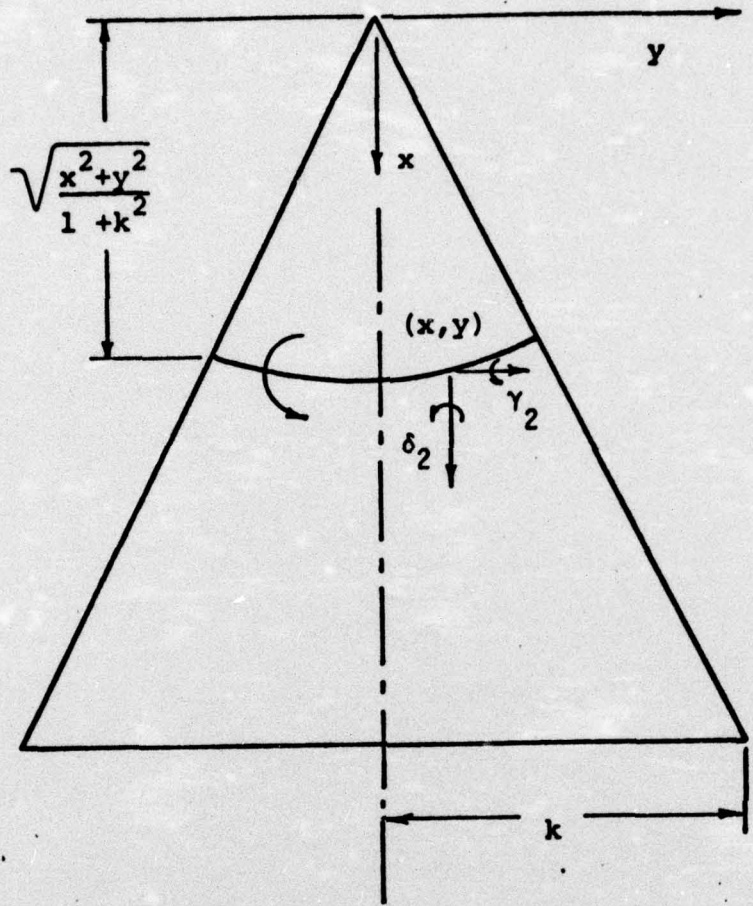
Finally, the location of the leading-edge vortex is defined by the polynomials

$$y_v = \sum_{\ell=1}^r g_{yv} x^\ell \quad (6)$$
$$z_v = \sum_{\ell=1}^r g_{zv} x^\ell$$

This introduces the final unknowns g_{yv} , g_{zv}

If there were no numerical difficulties associated with this problem, one could obtain improved accuracy by increasing the number of modes and, consequently, increasing the number of unknowns. However, for the given set where both the leading-edge vortex strength and vortex locations are defined by polynomials, a large number of modes also increases the problems related with the numerical analysis necessary to solve the resulting equations.

After the mode shapes have been defined, it is necessary to determine appropriate governing equations to determine the unknown coefficients.



$$\gamma_2(x, y) = \frac{x}{\sqrt{x^2 + y^2}} - \frac{d\Gamma_w(x_e)}{dx} x_e \sqrt{\frac{x^2 + y^2}{1 + k^2}}$$

$$\delta_2(x, y) = \frac{y}{\sqrt{x^2 + y^2}} \quad \frac{d\Gamma_w(x_e)}{dx} \quad x_e = \sqrt{\frac{x^2 + y^2}{1 + k^2}}$$

Figure 4. Representation of bound vorticity feeding leading-edge vortex.

The governing equations are the no-flow condition through the wing and the no-load condition on the free vortex sheet and on the leading-edge vortex-cut combination.

The downwash condition becomes

$$w = - \sin \alpha \quad (7)$$

where α is the angle of attack and w is the downwash induced by the vorticity distribution. This requires the evaluation of the w component of the integral in Equation 1 at a set of collocation points. The sinusoidal distribution of collocation points of Multhopp (1950)⁷ modified for the delta wing is given in Figure 5. A large amount of computational time is consumed by the calculation of the contribution from the wing surface since the denominator contains a singularity at the collocation points. Figure 6 gives the integration regions employed for the surface integration. Each region was covered by a 24x24-point Gaussian quadrature. Fortunately, this computation does not require any iterations.

The no-load condition on the trailing sheet is satisfied approximately. First, the Kutta condition at the trailing edge requires the vorticity vector to be parallel to the velocity vector.

$$\frac{\gamma(1,y)}{\delta(1,y)} \equiv \tan \beta = \frac{v}{\cos \alpha + u} \quad (8)$$

This equation is employed at collocation points along the trailing edge. Secondly, aft of the trailing edge, the wake is considered to be the same as in the linearized lifting surface theory, since the major cause of nonlinearity is the presence of the leading-edge vortices which induce

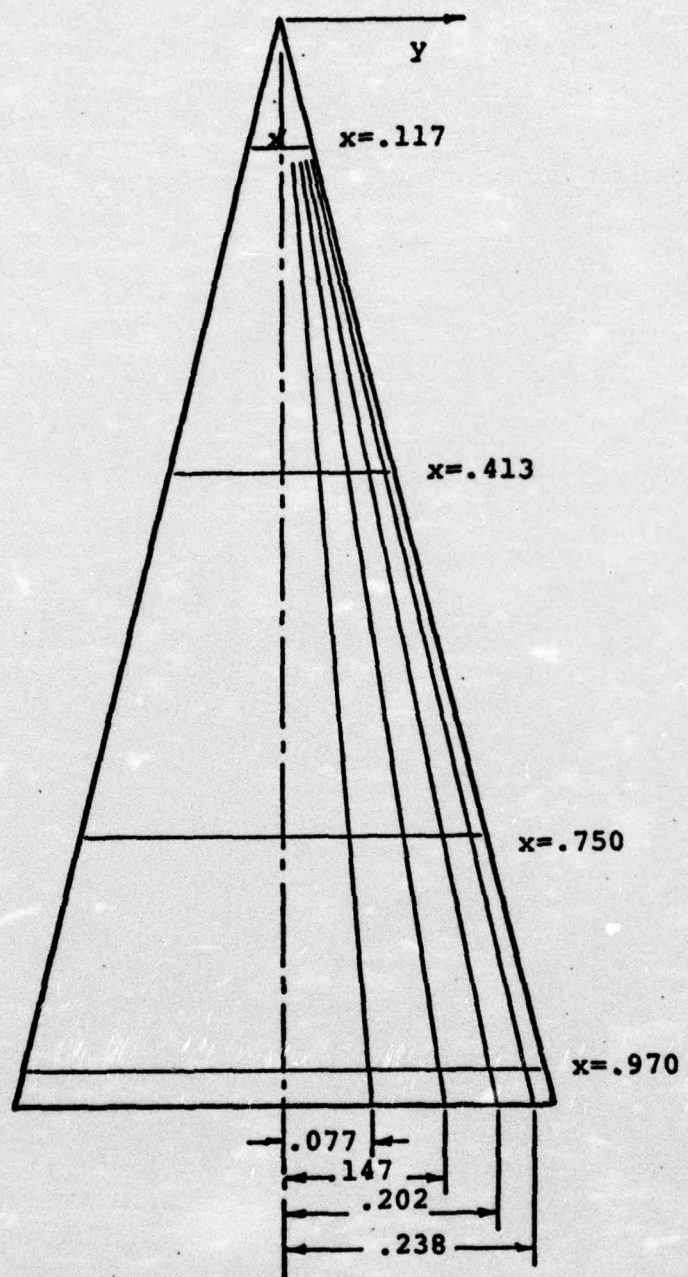


Figure 5. Wing collocation points.

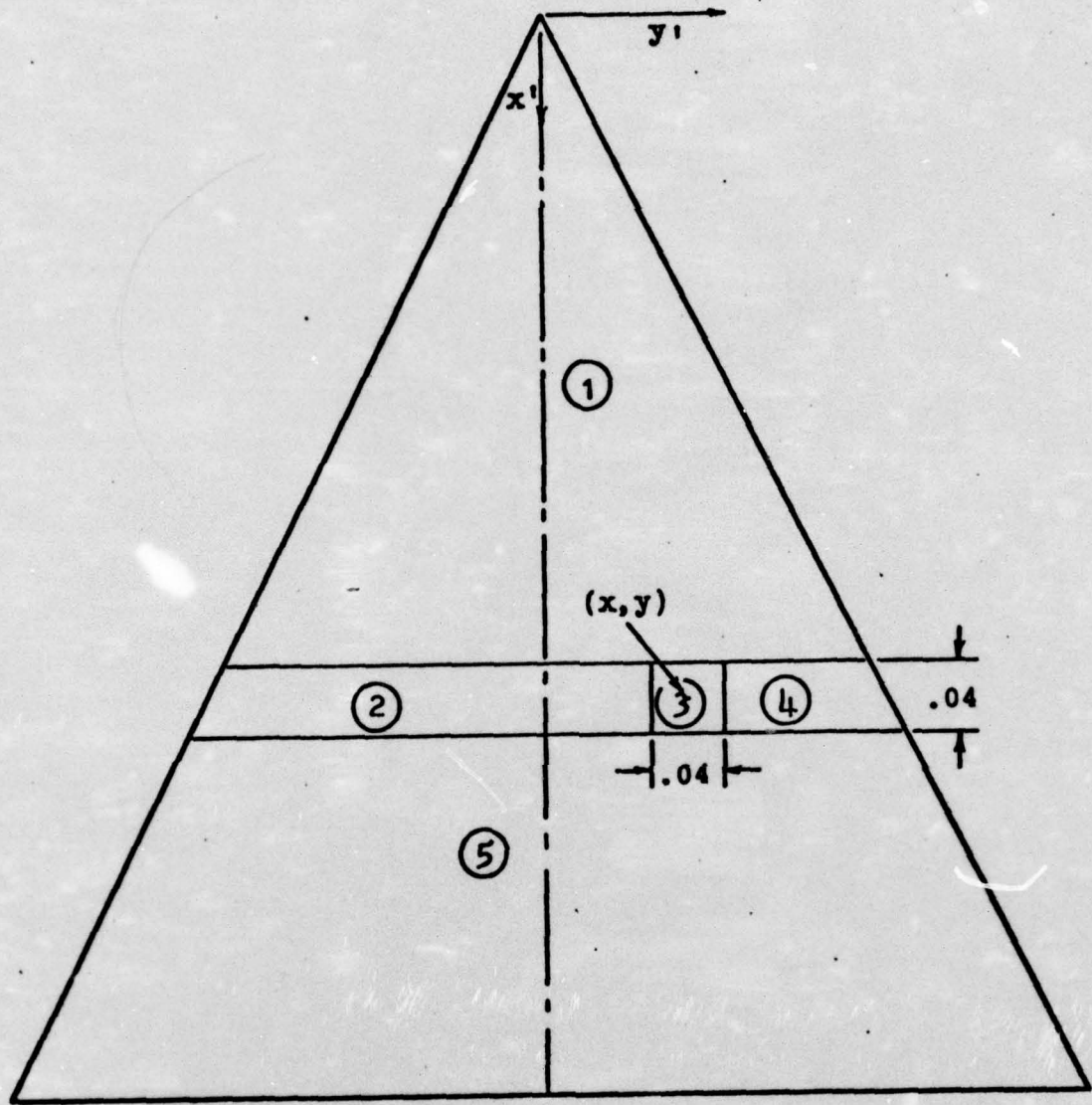


Figure 6. Regions of integration for upwash coefficients at point (x, y) .

high spanwise velocities on the planform.

Finally, the condition of no-load on the vortex cut is formulated on the right-hand vortex as an extension of the Brown and Michael model.

The force components in the y and z directions are given by F_y and F_z , respectively.

$$\begin{aligned} F_y &= -2\Gamma \left[\frac{dz_v}{dx} + \frac{1}{\Gamma} \frac{d\Gamma}{dx} z_v - w_1 - \sin\alpha \right] \\ F_z &= 2\Gamma \left[\frac{dy_v}{dx} + \frac{1}{\Gamma} \frac{d\Gamma}{dx} (y_v - kx) - v_1 \right] \end{aligned} \quad (9)$$

where w_1 , v_1 are the velocities induced by the vorticity distributions excluding the contributions of the right-hand vortex on itself. The calculations of the velocities v_1 and w_1 at collocation points along the leading-edge vortex again require the evaluation of the surface integral in Equation 1. The integrand is no longer singular and two 24x24-point Gaussian quadratures are applied over the wing surface.

The procedure to calculate the unknowns is now described. First, the number of modes to be employed must be specified. Once the number of modes and consequently, the number of unknown vorticity coefficients have been determined, it is necessary to choose an iterative scheme to satisfy the system of equations provided by the downwash condition, the Kutta condition and the no-force condition. For a given vortex location, the downwash condition is linear in terms of the vorticity distribution while the equations provided by the Kutta condition and the no-force condition are nonlinear in all parameters.

A preliminary formulation followed the procedure of Nangia and Hancock and only attempted to reduce the amount of computation involved during each step. Their method can be summarized as follows:

- 1) Evaluate the contributions to the downwash from the wing vorticity.
- 2) Specify the initial position of the vortex. For example, this can be furnished by the Brown and Michael model.
- 3) Specify an initial distribution of $\beta(y)$ such that it does not exceed $\tan^{-1}(y)$.
- 4) Evaluate the downwash integral due to the vortices and wake.
- 5) Formulate the Kutta condition as linear equations in the unknown vorticity distribution at the collocation points using the specified $\tan\beta$.
- 6) Solve the simultaneous equations from the downwash and Kutta conditions for the vorticity coefficients $a_{p,q}$ and g_q .
- 7) Use the results of the previous steps to determine new values for β .
- 8) If the new value of β is greater than or equal to the initial value in step 3), go on to the next step; for smaller values of β , iterate between 4) and 7) until the value of β converges. This conditional form for calculating β is employed, because Nangia and Hancock found that the procedure otherwise furnished unrealistic results.
- 9) Calculate the forces on the right-hand vortex using the assumed vortex position and the previously obtained vorticity distributions. If the force exceeds a prescribed tolerance, then the slopes of the new vortex location are calculated from

$$\frac{d}{dx} \Delta z_v = d \frac{F_y}{|F_y^2 + F_z^2|^{1/2}} \quad (10)$$

$$\frac{d}{dx} \Delta y_v = -d \frac{F_z}{|F_y^2 + F_z^2|^{1/2}}$$

where d is chosen small enough to prevent divergence of the method, e.g., $d = .01$. Since the forces have been normalized, the vortex movement is restricted to d .

10) Iterate between steps 4) and 9) until the forces become sufficiently small. The solution has then been obtained for the given flow conditions.

This original procedure has been modified in the present procedure so that the program can be run automatically with a minimum of stops to input new data.

Instead of specifying β in Step 3, the downwash condition was linearized with respect to the vorticity coefficients and the initial approximation for the coefficients $a_{p,q}$ and g_q are found directly from the downwash equations. Then β can be calculated by employing Equation 8.

The calculation of the forces F_y and F_z involve integrations over the wing surface to obtain the contribution to the v and w velocity components at the collocation points along the leading-edge vortex. Such integrations are time-consuming in the present scheme. Since a large number of iterations are required, a substantial savings could be gained by developing an iterative scheme with faster convergence.

In the two-dimensional theory of Brown and Michael, one encounters a similar problem in solving for the vortex location, y_v and z_v , in the cross-

flow plane by satisfying the no-force condition. Brown and Michael originally solved the problem indirectly by assuming values of the vortex location and satisfied the no-force condition by trial and error. Later, Pullin (1973) developed a Newton's method for the Smith type model, which included the Brown and Michael solution as a degenerate case. Trial runs of Pullin's program indicated that the Newton's method "converged" in approximately four iterations for the Brown and Michael model.

A Newton's method has several advantages over the Nangia and Hancock procedure. First, the scheme is amenable to automatic iteration without operator interference. Secondly, Newton's method has been shown to be successful for a wide variety of problems. The Nangia and Hancock procedure, on the other hand, has neither of these virtues. First, from Equation 10, the extent of the vortex movement is always 'd', which must be specified by the operator. Secondly, by comparing Equations 9 and 10, one sees that the Nangia and Hancock procedure for moving the vortex is equivalent to a Newton's method in which the velocities, v_1 and w_1 , are considered constant with respect to the vortex movement. The results of numerical experiments discussed in the next section indicate that the ignored derivatives are important. Consequently, although the Nangia and Hancock method appears to work for the simple case they considered, the procedure is not generally valid and has a convergence rate which depends on the applicability of the procedure and the judgment of the operator in selecting values for 'd'. Therefore, a Newton's method was developed to locate the new vortex position from the forces calculated in the preceding iteration. This replaces step 9) in the Nangia and Hancock procedure.

Results of the Program

The problem was formulated for the unit aspect ratio delta wing at an angle of attack of 14.3° . Four spanwise modes and 5 chordwise modes were employed to describe the surface vorticity, since these were the number of modes employed by Nangia and Hancock. This choice for the vorticity representation corresponds to twenty unknown $a_{p,q}$'s and five g_q 's in Equation 4 for a total of twenty-five unknown vorticity coefficients. The initial location of the vortex was obtained from the conical, slender model of Brown and Michael. An approximation for the vorticity coefficients was then obtained by satisfying the downwash condition at twenty-five collocation points. These collocation points included the twenty interior points in Figure 5, as well as an intermediate row of five points at $x = .86$. This initial solution serves three primary purposes. First, it can be compared with the results of Brown and Michael and similar slender body theories to check the convergence of the method as a function of the number of modes. Secondly, it can provide insight on better choices for the vorticity functions. For example, in linearized lifting surface theory, the modes are chosen to approximate the two-dimensional flat plate results and the elliptic wing result. Unfortunately, it is more difficult to obtain such a simple choice of vorticity functions for a leading-edge vortex problem as the suction peak location is a function of the vortex core location, which is originally unknown. Hopefully, a better choice of vorticity functions can be developed in the future from the results of this investigation. Finally, this initial set of vorticity coefficients is required to calculate an initial choice of β , which is then used to formulate the quasi-linear form of the Kutta condition at the trailing edge from Equation 8.

The original results for the wing loading versus non-dimensionalized span are plotted in Figure 7 for two chordwise stations. These results are also compared with those of the Brown and Michael model for the equivalent aspect ratio and angle of attack. The present calculated values are similar to the slender body results but the loading decreases towards the trailing edge as a result of the finite planform.

Secondly, the Kutta condition was applied at the five collocation points at the trailing edge in Figure 5. The downwash condition previously applied at the twenty interior collocation points was used with the five new equations to provide enough constraints to calculate the new set of twenty-five unknown coefficients. The resulting loading distributions are shown in Figure 8. Note that the loading goes to zero at the trailing edge in this model which is not possible in slender body models. Also, note the peaks in the loading which are not possible in linearized models. Some features of the model can be observed by examining a plot of the leading-edge vortex strength for the same case in Figure 9. Strictly speaking, $\frac{d\Gamma}{dx}$ should be zero at the trailing edge in this model, since the leading edge vortex is only fed along the leading edge of the planform. This condition was included in a later run, but since it only affected the shape of the curve near the trailing edge, this constraint was not incorporated in this early model. However, in later models, when the force is to be calculated at points near the trailing edge, this imposed boundary condition becomes important and would be best handled by a choice of modes which incorporated this condition automatically. Although the magnitude of the leading-edge vortex strength changed only slightly with the application of the Kutta condition, the functional shape became more pronounced. Numerical experiments were conducted

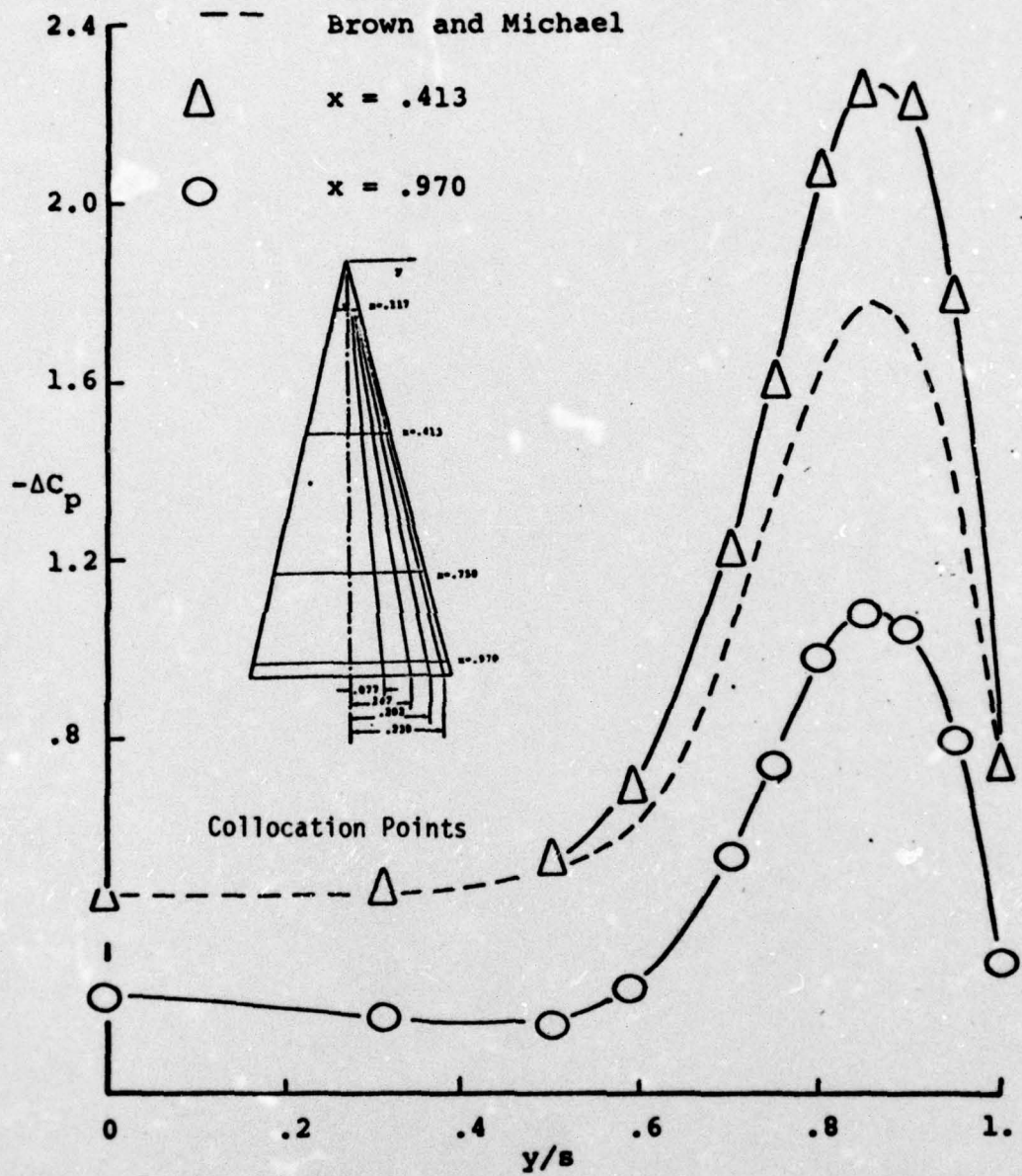


Figure 7. Loading calculated by satisfying downwash condition only. Symbols indicate points where pressure was calculated. 25 combined modes.

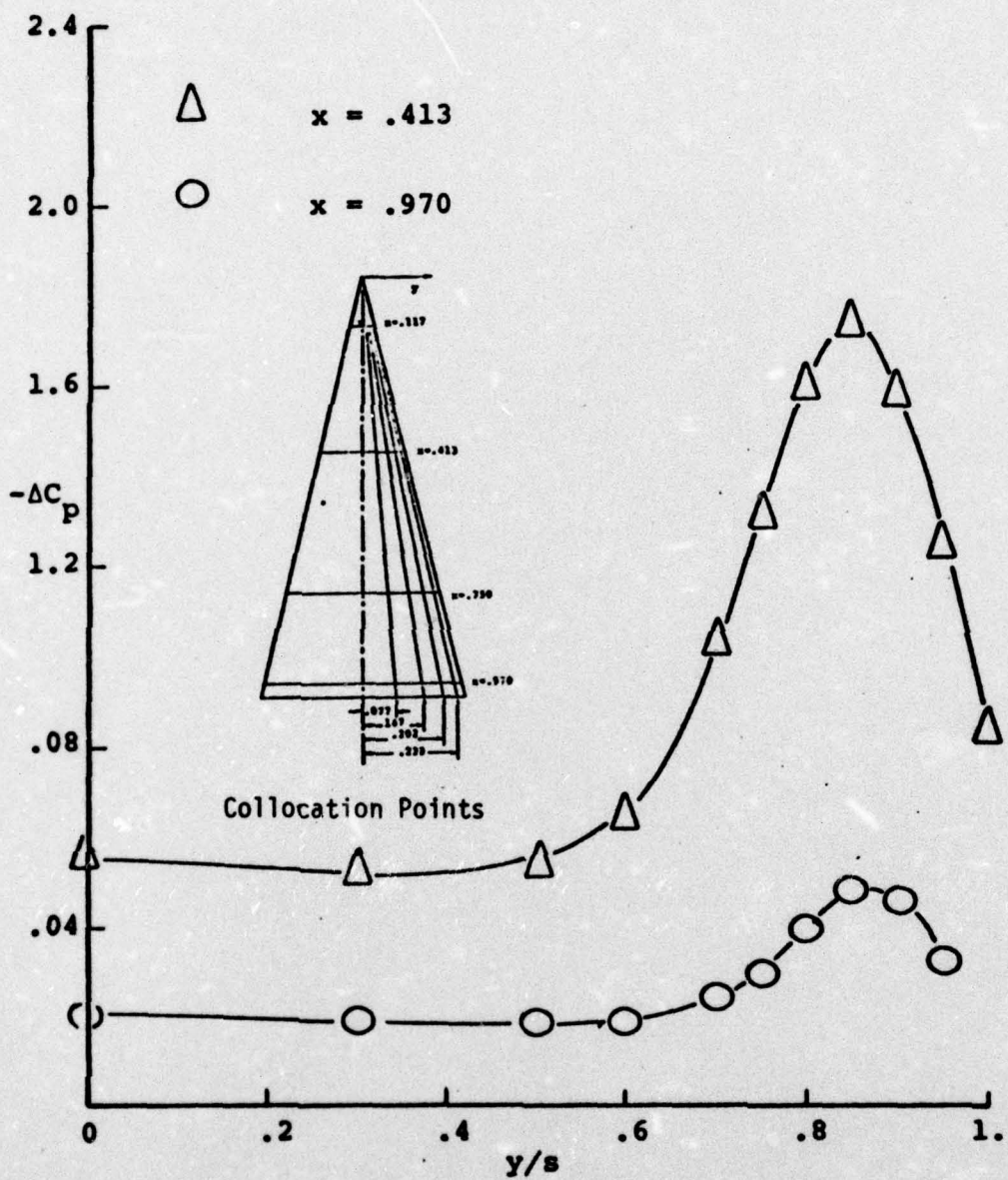


Figure 8. Loading calculated by satisfying downwash and Kutta conditions. 25 modes.

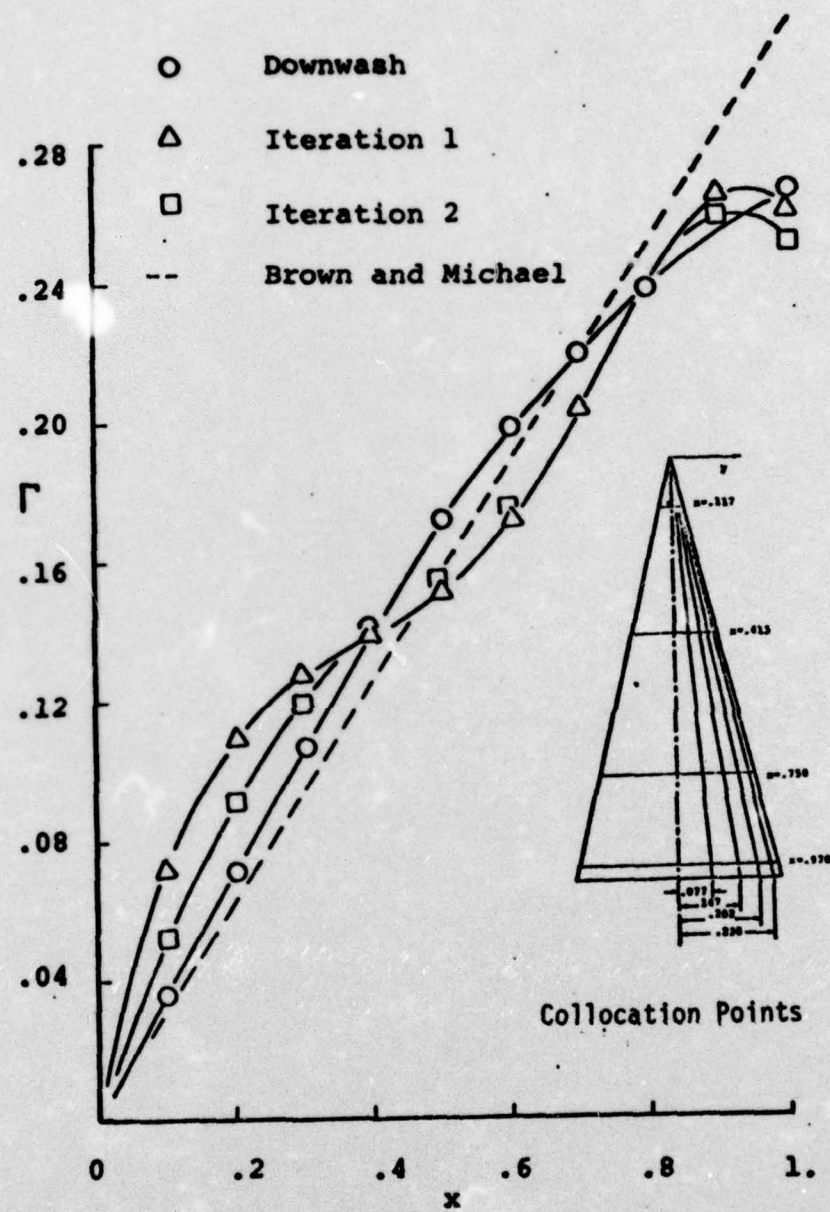


Figure 9. Leading-edge vortex strength. Iterations 1 and 2 refer to number of applications of the Kutta condition. 25 combined modes.

to demonstrate that the curvature of the function representing the vortex strength was not a numerical error or a result of the collocation points. Rather, it is a feature of the present formulation which is alleviated by further iterations.

Preliminary results indicated large values with alternating signs for the unknown vorticity coefficients, which suggest several difficulties. First, there is the loss of significant figures in the final answer when two large numbers are differenced to obtain a small number. Secondly, they indicate that the original choice of vorticity functions was probably not a good one. Finally, their values can change radically from one iteration to the next. This is important, since one could save considerable computational effort if a quasi-linearization could be employed about some initial value. For example, it may be possible to ignore some of the derivatives in the Jacobian or, for slow variations, some nonzero terms may only have to be calculated once for several iterations.

The present set of equations for the unknown vorticity coefficients is also sensitive to small perturbations in the boundary conditions. This is due to the fact that the relatively large matrix, 25x25, is not diagonally dominant, which causes numerical difficulty in the solution procedure.

To reduce these numerical difficulties and decrease the computational effort, it would be advantageous to utilize the minimum number of modes which would adequately describe the spanwise loading distribution. Therefore, the computer program developed to calculate the vorticity coefficients from the downwash condition was used to approximately determine the minimum number of spanwise modes.

This was done by using a quasi-conical model where only the linear chordwise modes were retained in the set of vorticity functions. The location

of the leading-edge vortex was taken from the Brown and Michael model and should, therefore, satisfy the no-force condition. This model is quasi-conical, in the sense that the integration is terminated at the trailing edge of this subsonic model and is not extended to infinity. The results of these calculations should only match the Brown and Michael solutions approximately. The pressure distribution obtained using three and four spanwise modes and twenty interior collocation points in a least-square method is compared with the conical model in Figure 10. The leading-edge vortex strength, which is now linear, is compared in Figure 11. These results indicate that four spanwise modes are sufficient to adequately describe the spanwise loading distribution with the given choice of loading functions.

A similar study was not conducted to determine the minimum number of chordwise modes, because the original modes, given in Equation 4, behave like simple polynomials in chordwise direction. Such polynomials are associated with loss of accuracy, and attention was focused on attempting to develop a better chordwise dependence rather than determining their minimum. However, if these original chordwise modes were to be used, a least squares method should be employed to reduce this problem.

Finally, a program was developed to calculate the forces on the vortex and to move the vortex according to Equation 10. This program required approximately one minute to calculate the forces at five chordwise stations. To prevent divergence, the movement had to be small which implied a large number of iterations. Therefore, a procedure more amenable to automatic iteration was sought.

Thus, a numerical experiment on the applicability of Newton's method was conducted for the two-dimensional model of Brown and Michael, since it was felt that useful information could be obtained on the force Jacobian

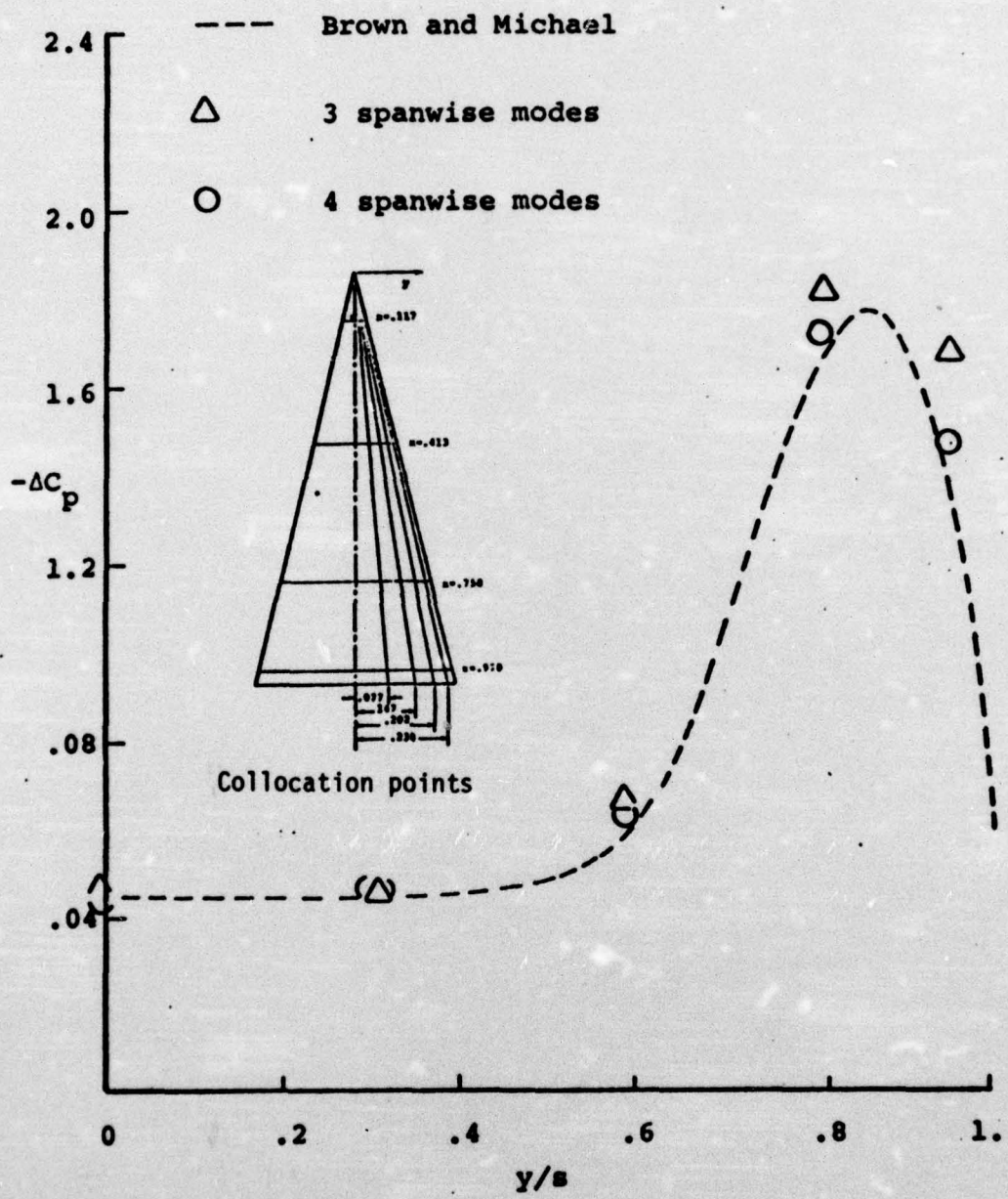
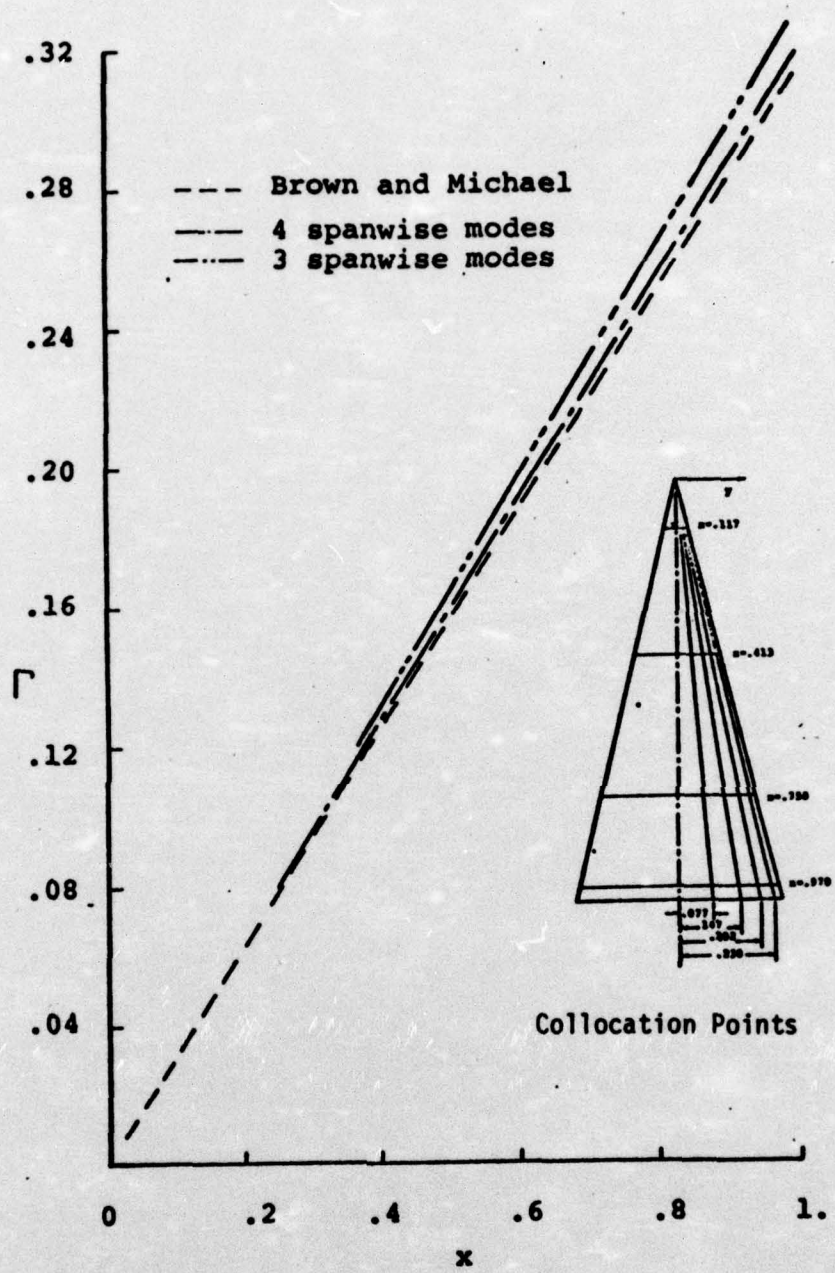


Figure 10. Pressure distribution for 3 and 4 spanwise modes.



**Figure 11. Leading-edge vortex strength
for 3 and 4 spanwise modes.**

more economically in two dimensions than in the fully three-dimensional case. The numerical experiment was conducted on a slender delta wing of the same aspect ratio and angle of attack as in the present case for different leading-edge vortex strengths and locations which correspond to the unknowns in the present case. Equation 9 was employed to calculate the forces, F_y and F_z . In the conical Brown and Michael model, both the vortex location, y_v and z_v , and the vortex strength, Γ , are linear in the chordwise variable.

Results of this experiment for $\Gamma(1.) = .31$ are plotted in Figure 12 for the spanwise force, F_y , and in Figure 13 for the vertical force, F_z . The forces are plotted versus vortex location, y_v and z_v , at $x = 1$. The triangle symbol represents the point where the lines, $F_y = 0$ and $F_z = 0$, intersect to define the stable location for this flow condition. The two-dimensional results indicate that F_z is monotonic as a function of both y_v and z_v . F_y , on the other hand, is monotonic over much of the plane, but is poorly behaved near the leading-edge. This did not preclude the use of Newton's method on the Brown and Michael model, but may prove to be a problem in the three-dimensional case, since Newton's method is based on a linear approximation. However, it should be possible to minimize this problem by avoiding this region or by suppressing some of the derivatives or by limiting changes of the leading-edge vortex location to one axis at a time.

Therefore, a Newton's procedure was developed for the three-dimensional case to calculate the new location of the vortex based on the forces calculated in the preceding iteration. This modification improved the rate of convergence for the reduction of the forces for a given vorticity distribution. However, when the given vorticity distribution was altered

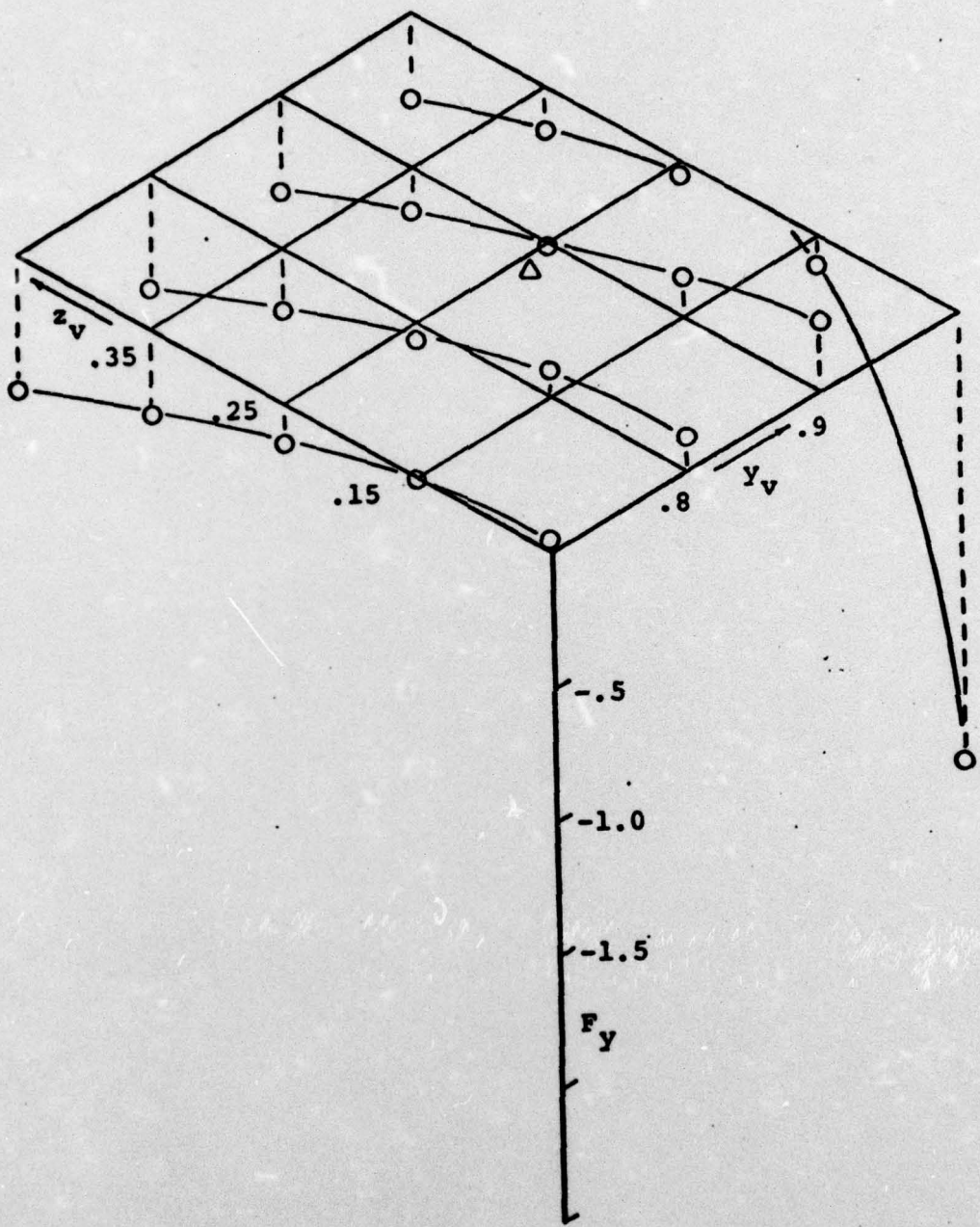


Figure 12. Spanwise force, F_y , on right-hand vortex for $\Gamma(1)=.31$.

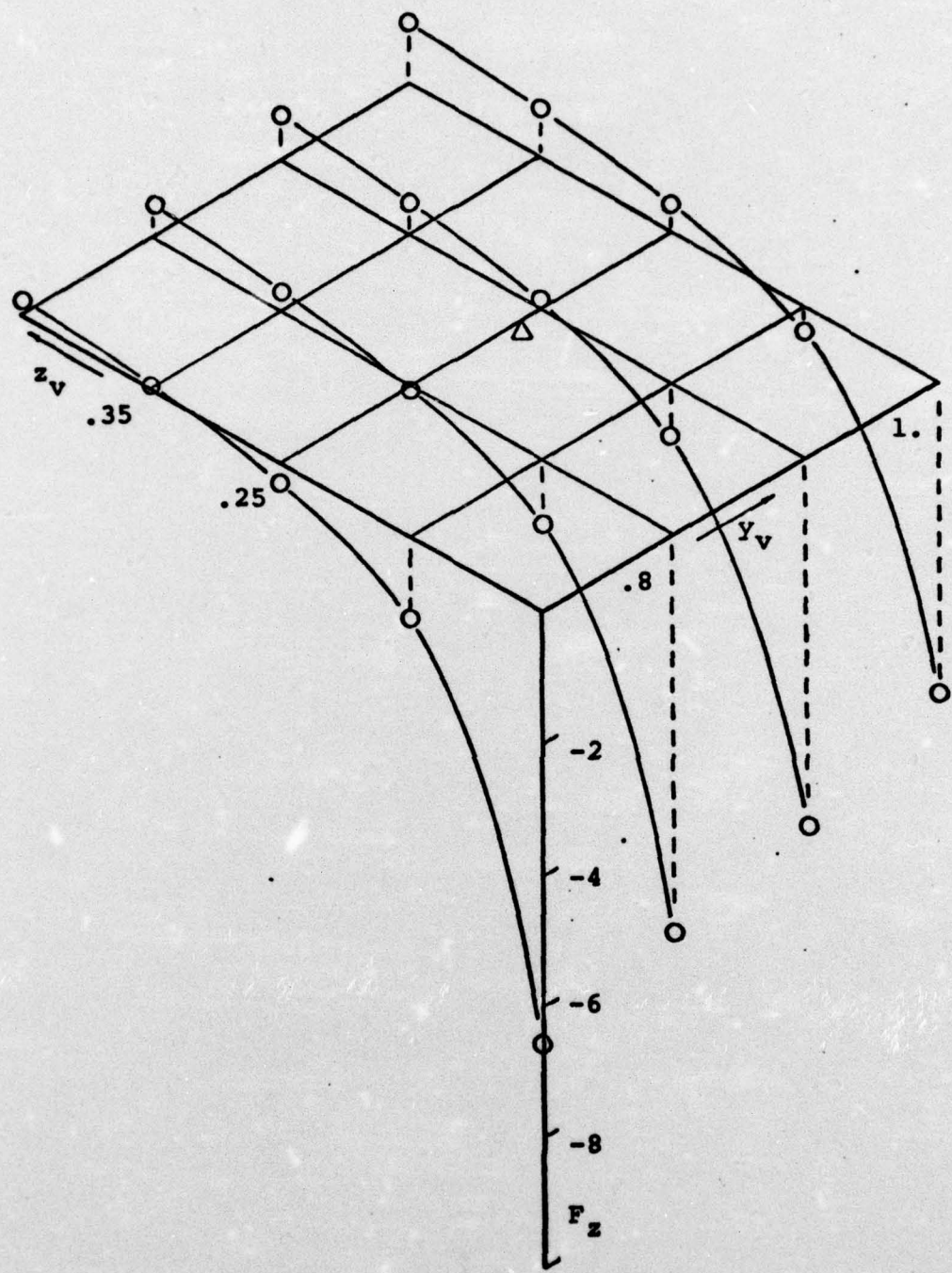


Figure 13. Vertical force, F_z , on right-hand vortex for $\Gamma(1) = .31$.

by iterating on the downwash and Kutta conditions, the large changes in the vorticity coefficients neutralized much of the gain in the convergence rate. A large number of iterations were therefore not conducted, because a more economical computing procedure must be developed before this method can be used economically. As is, the program will produce answers for the delta wing problem given an initial vortex location and outputs from supplementary programs which calculate the downwash contribution from the wing and an initial approximation for the leading-edge vortex strength.

Conclusion

In conclusion, further effort should be devoted to model the leading-edge vortex problem for arbitrary planforms by a continuous vorticity model with unknown coefficients, since the role of vortex-wing interactions becomes increasingly crucial for high technology aircraft. The present procedure can be easily generalized to arbitrary planforms and include arbitrary sources of free vortices, but is restricted by the computational effort.

Due to the advance of computational power and some minor refinements employed in these calculations, the calculation of the downwash contribution from the wing has been reduced from the two and a half hours on an Atlas⁶ to twelve minutes for twenty collocation points and 25 unknown vorticity coefficients on an IBM 370-168. This downwash calculation need only be performed once for a given planform and a given set of collocation points, and solutions can then be obtained for all angles of attack and for different models of the trailing wake, leading-edge vortex, and leading-edge vortex sheet. Thus, it was originally considered justified to devote this much effort to this downwash calculation, since it was implied by Nangia and

Hancock that this calculation would require the major portion of computational effort. However, the present investigation indicates that the program for reducing the forces while satisfying the downwash and Kutta Conditions consumes an equivalent or even greater effort. Therefore, an important conclusion is that several important modifications must be utilized to make the present program generally useful. Primarily, it would be desirable to reduce the order of the matrices in terms of the numerical instabilities and to further reduce the computational effort to improve the versatility of the method. This would involve improved choices for the vorticity functions, the use of a least squares method, and an alternate formulation of the integral equation.

Presently, four spanwise modes of the Nangia and Hancock type adequately describe the spanwise loading. However, due to the large values of the coefficients with alternating signs, better accuracy can probably be obtained by choosing more orthogonal functions, which retain the square root behavior near the leading edge. On the other hand, the chordwise variation must be altered to satisfy the $d\Gamma/dx = 0$ condition at the trailing edge and to eliminate the numerical difficulties associated with simple polynomials.

The least-squares method, mentioned in connection with determining the minimum number of spanwise modes, is an important technique for alleviating some of the numerical difficulties associated with large coefficients of alternating sign and with large matrices. The least-squares technique does not attempt to solve the set of simultaneous equations at a finite number of collocation points exactly. Instead, the number of collocation points is chosen to be greater than the number of unknowns, and the problem is formulated to minimize the error at all points. This type of formulation results in smoother solutions, i.e., smaller values of coefficients, and tends to minimize local anomalies. This method also allows a smaller number of modes to

be utilized to adequately predict the flow characteristics. Finally, the least-squares procedure results in a more diagonally dominant matrix than can be obtained by simply applying the boundary conditions.

Finally, an alternate formulation of the integral equation is suggested. Basically, the vorticity which does not feed the leading-edge vortex can be represented by a vorticity distribution borrowed from a linear lifting surface theory. Such integrations in lifting surface theory routinely require less than a minute, and this alteration would drastically reduce the amount of computational effort required to calculate the velocity contributions from the surface vorticity.

These modifications have been suggested by the results of the present investigation, and their successful implementation would greatly enhance the versatility of a three-dimensional lifting surface theory with leading-edge vortices.

REFERENCES

1. Matoi, T. K., "On the Development of a Unified Theory for Vortex Flow Phenomena for Aeronautical Applications," MIT Report, AD No. A012399, 1975.
2. Örnberg, T., "A Note on the Flow around Delta Wings," KTH Aero TN 38, RIT, 1954.
3. Brown, C. E., and Michael, W. H., "On Slender Delta Wings with Leading-Edge Separation," NACA TN 3430, 1955.
4. Smith, J. H. B., "Improved Calculations of Leading-Edge Separation from Slender Delta Wings," RAE TR 66070, 1966.
5. Smith, J. H. B., "A Theory of the Separated Flow from the Curved Leading Edge of a Slender Wing," ARC R&M No. 3116, 1957.
6. Nangia, R. and Hancock, G. J., "A Theoretical Investigation for Delta Wings with Leading-Edge Separation at Low Speeds," ARC CP No. 1086, 1968.
7. Multhopp, H., "Methods for Calculating the Lift Distribution of Wings (Subsonic Lifting-Surface Theory)", ARC R&M No. 2884, 1950.
8. Pullin, D. I., "A Method for Calculating Inviscid Separated Flow about Conical Slender Bodies," ARL/A14, Australian Defense Scientific Service, Rep. 140, 1973.

SYMBOLS

a	vorticity coefficient related to surface vorticity only
c	chord; all lengths are nondimensionalized by chord
d	scale factor to limit movement of vortex
F	force on right-hand vortex
g	vorticity coefficient related to leading-edge vortex
i	unit vector in x-direction
j	unit vector in y-direction
k	unit vector in z-direction; semispan at trailing edge
l	dummy index
p	dummy index
q	dummy index
r	radius vector from origin
S	surface of integration
U	free stream velocity; all velocities are nondimensionalized by U
u	perturbation velocity component in x-direction
v	perturbation velocity in y-direction; vector v is total perturbation velocity
w	perturbation velocity component in z-direction
x	chordwise coordinate
y	spanwise coordinate; with subscript v, represents leading-edge vortex location
z	vertical coordinate; with subscript v, represents leading-edge vortex location

SYMBOLS (continued)

- α angle of attack
- β shedding angle at trailing edge
- γ spanwise vorticity component; vector γ is total vorticity
- Γ leading-edge vortex strength
- δ chordwise vorticity component

DISTRIBUTION LIST

Chief of Naval Research Department of the Navy Arlington, VA 22217 ATTN: Vehicle Technology Program Code 211	Defense Documentation Center Cameron Station, Bldg 5 Alexandria, VA 22314	12
Chief of Naval Development Department of the Navy Washington, DC 20360 ATTN: NAVMAT 0331 NAVMAT 0334	5 Department of the Army DCS for Research Development and Acquisition Washington, DC 20310 ATTN: DAMA-WSA (Mr. R. L. Ballard)	1
Naval Air Systems Command Department of the Navy Washington, DC 20361 ATTN: NAVAIR 320D NAVAIR 5301 NAVAIR 53013	1 U. S. Army Material Command 5001 Eisenhower Avenue Alexandria, VA 22333 ATTN: AMCRD-F	1
David Taylor Naval Ship Research & Development Center Aviation and Surface Effects Department Bethesda, MD 20084 ATTN: Code 16 Code 522.3	1 Director, Headquarters U. S. Army Air Mobility R&D Lab. Ames Research Center Moffett Field, CA 94035	1
Naval Research Laboratory Washington, DC 20375 ATTN: Technical Information Office, Code 2627 Library, Code 2629	1 Director, Ames Directorate U. S. Army Air Mobility R&D Lab. Ames Research Center Moffett Field, CA 94035	1
Superintendent U. S. Naval Academy Annapolis, MD 21402	6 Director, Langley Directorate U. S. Army Air Mobility R&D Lab	1
Superintendent U. S. Naval Postgraduate School Monterey, CA 93940	3 Langley Research Center Hampton, VA 23665	1
U. S. Naval Air Development Center Warminster, PA 18974 ATTN: Aeromechanics Department	1 Director, Eustis Directorate U. S. Army Air Mobility R&D Lab Fort Eustis, VA 23604	1
Commandant of the Marine Corps Washington, DC 20380 ATTN: Dr. A. L. Slafkosky Scientific Advisor, (Code RD-1)	1 U. S. Air Force Flight Dynamics Laboratory Wright-Patterson AFB, OH 45433 ATTN: PT, Prototype Division FGC, Control Criteria Branch FXM, Aeromechanics Branch	1
	1 Air Force Office of Scientific Research 1400 Wilson Boulevard Arlington, VA 22209 ATTN: Mechanics Division	1

National Aeronautics and Space Administration 600 Independence Avenue, SW Washington, DC 20546 ATTN: Code RAA Code RAV	1	Lockheed Missiles & Space Co., Inc. Huntsville Research & Engineering Center P. O. Box 1103 Huntsville, AL 35807 ATTN: Mr. A. Zalay	1
National Aeronautics and Space Administration Ames Research Center Moffett Field, CA 94035 ATTN: Large-Scale Aerodynamics Branch	1	Rochester Applied Science Associates 1055 J. Clyde Morris Boulevard Newport News, VA 23602 ATTN: Mr. Richard P. White	1
National Aeronautics and Space Administration Langley Research Center Hampton, VA 23665 Subsonic, Transonic Aerodynamics Division ATTN: James F. Campbell	1	Lockheed-Georgia Company Department 72-74, Zone 403 Marietta, GA 30063 ATTN: Mr. Charles Dixon	1
Commander, Air Force Plant Representative Office Lockheed-Georgia Company Marietta, GA 30060	1	Sage Action, Inc. P. O. Box 416 Ithaca, N.Y. 14850 ATTN: Dr. D. E. Ordway	1
Office of Naval Research Department of the Navy Arlington, VA 22217 ATTN: Mr. M. Cooper, Code 430B	1		
Office of Naval Research Branch Office 495 Summer Street Boston, MA 02210 ATTN: Dr. A. D. Wood	1		
ONR Branch Office Chicago 536 South Clark Street Chicago, IL 60605 ATTN: Mr. M. A. Chaszeyka	1		
Texas A&M Research Foundation Texas A&M University F. E. Box H College Station, TX 77843 ATTN: Dr. B. M. Rao	1		